Electronic Supplementary Material (ESI) for Physical Chemistry Chemical Physics.
This journal is © the Owner Societies 2020

Supporting information for:

Enhanced Extraction of Phenol from Model Oils Using Ionic Liquids Elucidated with Neutron Diffraction

Adam H. Turner,[*,†,‡] Emily Byrne,[†] Thaise Pereira,[†] and John D. Holbrey[*,†]

† *The QUILL Research Centre, School of Chemistry and Chemical Engineering, The Queen's University of Belfast, Belfast BT9 5AG, UK*

‡ *Department of Chemistry, Ateneo de Manila University, Quezon City 1108, Philippines*

E-mail: aturner@ateneo.edu; j.holbrey@qub.ac.uk

Table S1: Matrix of how proposed changes to the ionic liquid are expected to effect their interaction properties

		Cation Electron Density	
		Low	High
Anion Basicity	Low	[Me – Py][NTf_2]	[Me – 3-Pic][NTf_2]
	High	[Me-Py][OTf]	[Me-3-Pic][OTf]

Synthesis and Procedures

Synthesis of $[NTf_2]^-$ Ionic Liquids

N-methylpyridinium *bis*{(trifluoromethyl)sulphonyl}imide was synthesised as previously outlined.[S1]

Using an inert atmosphere (N_2), dimethylsulphate (10 g, 81 mmol) was added dropwise to pyridine (6.1 g, 77 mmol) in a round-bottomed flask maintained at 50 °C with stirring. Care was taken during the addition to ensure temperature increases were kept to a minimum as the product is temperature sensitive. After cooling the reaction mixture to room temperature, the product was used without further purification for metathesis.

Metathesis was done with aqueous solutions of Li[NTf_2] (21.5 g, 75 mmol) and *N*-methylpyridinium methylsulphate (15.3 g, 71 mmol) in 35 mL H_2O. *N*-methylpyridinium *bis*{(trifluoromethyl)sulphonyl}imide was immediately produced by precipitation as a dense colourless hydrophobic liquid that crystallised on standing to form a white solid. The salt was collected by filtration, air drying, followed by in vacuo.

Synthesis of $[OTf]^-$ Ionic Liquids

Inside a glovebox, methyltrifluoromethane sulphonate (5 g, 30 mmol) was added dropwise to pyridine (2.3 g, 29 mmol) with stirring at 25 °C with care taken to ensure the solution did not overheat and cause the pyridine to evaporate. The sample was used directly for experimentation.

Sample Preparation

In a representative example, phenol (0.61 g, 6.5 mmol) was added to *N*-methylpyridinium *bis*{(trifluoromethyl)sulphonyl}imide (5 g, 13 mmol) under an inert atmosphere in a glove box, and heated to 60 °C. Initially the samples were combined such that a 2:1 IL:phenol ratio would be produced but in the case of the [Me–Py][NTf_2] system, after equilibration, a precipitate formed, through ^{1}H-NMR, it was found that the actual solution composition was $\chi_{Phenol} = 0.34$ or 34 % phenol.[S1] Cooling to room temperature results in further precipitation of the ionic liquid producing a sample of 38 mol % phenol. This phenomena was not observed for the $[OTf]^-$ ionic liquids.

Figure S1: Figure showing the eutectic liquid formed at room temperature formed between [Me−Py][NTf$_2$] and phenol in a 2:1 molar ratio. IL (left), IL:phenol (middle), and phenol (right) at 20 °C.

Gas Chromatography Analysis

Gas chromatography (GC) analysis (Agilent 7820A) with flame ionisation detection (FID) fitted with a HP-5 column with dimensions of 30 m$\times$320 μm, particle size 0.25 μm. The mobile phase was hydrogen at a flow rate of 30 mL min^{-1} and air at a flow rate of 400 mL min^{-1} with a makeup flow of 25 cm^3/min of helium. The oven temperature was set at 350 °C and the sample size was 1 μL. Extraction efficiency was determined by difference between phenol content in the model oil before, and after, contacting with the organic salts, calibrating the GC response to an internal dodecane standard (0.01 M).

The final phenol concentration in the model oil was calculated by dividing ratio of phenol to dodecane peak areas by the gradient of the calibration curve previously obtained and the extraction efficiency calculated by comparing the initial and final phenol concentrations in the oil.

Phenol extraction from model oils with $[NR_4]X$ (X = Cl, Br, I) salts

Table S2 shows phenol extraction efficiency from hexane and toluene as model aliphatic and aromatic phases using tetraalkylammonium halide salts ($X = Cl^-, Br^-, I^-$) as eutectic liquid-formers. The effects of alkyl chain substitution in $[NR_4]Cl$ salts is largely masked for phenol recovery from aliphatic hexane (Fig. S2 due to the strong and dominant influence of the chloride anion. Examining the corresponding iodide salts illustrates how, when phenol–anion HBD-HBA association is weakened, due to the reduced electronegativity of the anion,[S2] the increase in pi-cation association comes into play,[S3,S4] and the effect of alkyl chain length is more apparent. Phenol extraction efficiency, shown in Figs. S2 and S3 follows trend where extraction efficiency increases with increasing alkyl chain length ($[NMe_4]^+ < [NEt_4]^+ < [NPr_4]^+ < [NBu_4]^+$ (7%, 74%, 89% and 96% efficiency respectively), and decreases for a given cation with the increase in size, polarisibility and softness of the anion (Fig. S3).

Table S2: Phenol extraction efficiency (/% removed) from hexane and toluene model oils (Conditions,: hexane or toluene model oil, initial phenol concentration, 0.1 M, stirring time, 30 min, salt:phenol ratio 1:1, 30 °C)

Cation	Anion	Hexane	Toluene
$[NMe_4]^+$	Cl	90	
	Br		
	I	7	
$[NEt_4]^+$	Cl	100	95
	Br	98	77
	I	74	8
$[NPr_4]^+$	Cl	100	
	Br		
	I	89	
$[NBu_4]^+$	Cl	100	
	Br		
	I	96	

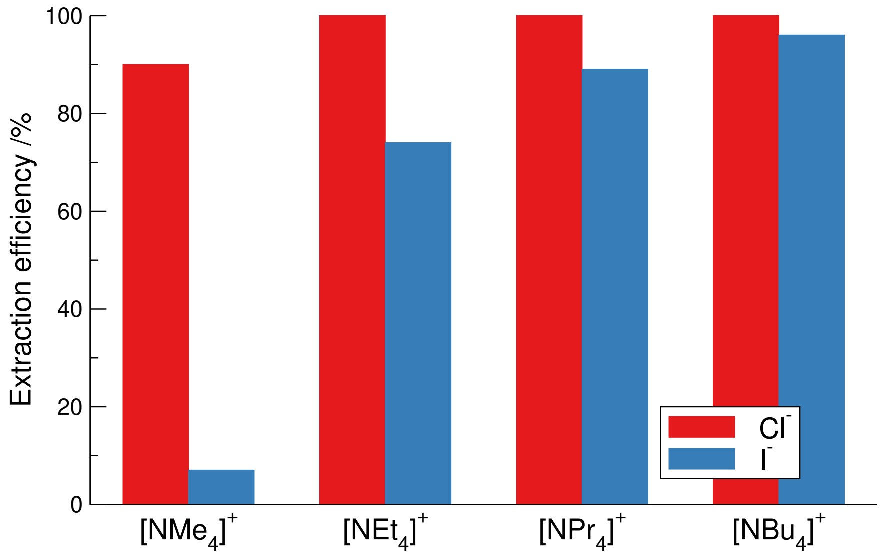

Figure S2: Effect of alkyl chain length on phenol extraction efficiency from hexane with tetraalkylammonium chloride and iodide salts; $[NMe_4]^+$, $[NEt_4]^+$, $[NPr_4]^+$, and $[NBu_4]^+$. Conditions: hexane model oil, initial phenol concentration, 0.1 M, stirring time, 30 min, salt:phenol ratio 1:1, 30 °C.

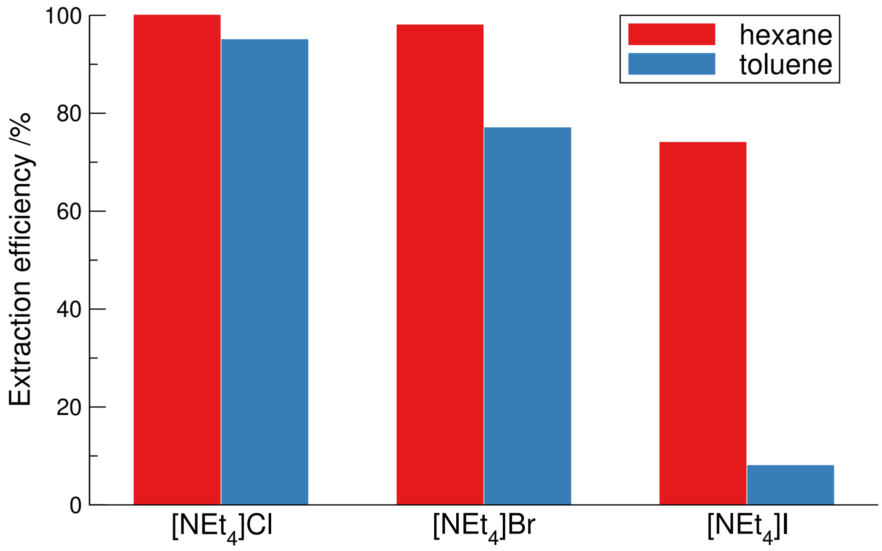

Figure S3: Effect of anion on phenol extraction from hexane and toluene with tetraethylammonium halide salts; $[NEt_4]Cl$, $[NEt_4]Br$, and $[NEt_4]I$. Conditions: initial phenol concentration, 0.1 M, stirring time, 30 min, salt:phenol ratio 1:1, 30 °C.

EPSR Parameters

Table S3: Lennard-Jones (ε and σ) and charge (q) parameters used for the reference potential of the Empirical Potential Structure Refinement model for anions derived from the literature.[S5,S6]

Atom type	ε (kJ mol^{-1})	σ (Å)	q (e)
$[NTf_2]^-$			
N	0.7113	3.25	-0.66
S	1.0460	3.55	1.02
O	0.8786	2.96	-0.53
C	0.2761	3.50	0.35
F	0.2218	2.95	-0.16
$[OTf]^-$			
S	1.0460	3.55	1.02
O	0.8786	2.96	-0.63
C	0.2761	3.50	0.35
F	0.2280	2.95	-0.16

Table S4: Lennard-Jones (ε and σ) and charge (q) parameters used for the reference potential of the Empirical Potential Structure Refinement model for phenol and cations derived from the literature,[S1,S7] and OPLS-AA.[S8]

Atom type	ε (kJ mol^{-1})	σ (Å)	q (e)
Phenol			
CP1	0.800	3.70	0.1500
CP2	0.800	3.70	-0.1150
CP3	0.800	3.70	-0.1150
CP4	0.800	3.70	-0.1150
HP2	0.000	0.00	0.1150
HP3	0.000	0.00	0.1150
HP4	0.000	0.00	0.1150
OP	0.650	3.10	-0.5850
HPO	0.000	0.00	0.4350
[Me-Py]$^+$			
NR1	0.711	3.25	0.1824
CR2	0.293	3.55	0.0397
CR3	0.293	3.55	-0.2503
CR4	0.293	3.55	0.1304
HR	0.000	0.00	0.1863
CM	0.000	3.55	-0.3979
HM	0.000	0.00	0.1916
[Me-3-Pic]$^+$			
NR1	0.711	3.25	0.1800
CR2	0.293	3.55	-0.2115
CR3	0.293	3.55	0.2800
CR4	0.293	3.55	-0.1502
CR5	0.293	3.55	-0.1143
CR6	0.293	3.55	-0.1012
HR	0.000	0.00	0.2036
CM	0.293	3.55	-0.3865
HM	0.000	0.00	0.1853
CL	0.293	3.55	-0.4836
HL	0.000	0.00	0.1644

Table S5: Intramolecular bond distance (Å) and bond-angle (°) constraints used to define the basic structure of phenol and *N*-methylpyridinium cation in the initial EPSR simulation model derived from the literature,[S1,S7] and OPLS-AA.[S8]

Bond Distance	(Å)	Bond Angle	(°)
Phenol			
CP2–CP1	1.40000	CP3–CP4–CP3	120.0
CP2–CP3	1.40000	CP3–CP4–HP	120.0
CPX–HP	1.08000	CP1–CP2–CP3	120.0
CP1–OP	1.36400	CP1–CP2–HP	120.0
CP3–CP4	1.40000	CP3–CP2–HP	120.0
OP–HPO	0.94900	CP2–CP1–CP2	120.0
		CP2–CP1–OP	120.0
		CP2–CP3–CP4	120.0
		CP2–CP3–HP	120.0
		CP4–CP3–HP	120.0
		CP1–OP–HPO	113.0
$[\text{Me-Py}]^+$			
CM–HM	1.07900	NR1–CR2–CR3	120.0
CR2–NR1	1.33700	NR1–CR2–HR	120.0
CR2–CR3	1.37200	CR3–CR2–HR	120.0
CRX–HR	1.07200	CR2–NR1–CR2	120.0
NR1–CM	1.48100	CR2–NR1–CM	120.0
CR3–CR4	1.38700	CR2–CR3–CR4	120.0
		CR2–CR3–HR	120.0
		CR4–CR3–HR	120.0
		NR1–CM–HM	109.5
		HM–CM–HM	109.5
		CR3–CR4–CR3	120.0
		CR3–CR4–HR	120.0

Table S6: Intramolecular bond distance (Å) and bond-angle (°) constraints used to define the basic structure of *N*-methyl-3-picolinium cation in the initial EPSR simulation model adapted from the literature[S7] using OPLS-AA.

Bond Distance	(Å)	Bond Angle	(°)
$[\text{Me-3-Pic}]^+$			
CR2–NR1	1.347	NR1–CR2–CR3	120.0
CR2–CR3	1.388	NR1–CR2–HR	120.0
NR1–CR6	1.346	CR2–NR1–CR6	120.0
NR1–CM	1.476	CR2–NR1–CM	120.0
CR3–CR4	1.399	CR2–CR3–CR4	120.0
CR3–CL	1.500	CR2–CR3–CL	120.0
CR6–CR5	1.383	NR1–CR6–HR	120.0
CR4–CR5	1.391	HR–CR6–CR5	120.0
CR2–HR	1.088	CR3–CR4–HR	120.0
CR4–HR	1.091	CR5–CR4–HR	120.0
CR5–HR	1.088	CR3–CL–HL	109.5
CR6–HR	1.089	HL–CL–HL	109.5
CL–HL	1.096	CR4–CR5–HR	120.0
CM–HM	1.093	CR4–CR5–CR6	120.0
		HR–CR5–CR6	120.0
		CR3–CR2–HR	120.0
		CR4–CR3–CL	120.0
		NR1–CR6–CR5	120.0
		NR1–CM–HM	109.5
		HM–CM–HM	109.5
		CR3–CR4–CR5	120.0
		CR6–NR1–CM	120.0

Table S7: Intramolecular bond distance (Å) and bond-angle (°) constraints used to define the basic structure of *bis*{(trifluoromethyl)sulfonyl}imide and triflate anions in the initial EPSR simulation model derived from the literature.[S1,S5,S6]

Bond Distance	(Å)	Bond Angle	(°)
OLD $[NTf2]^-$			
C–S	1.81396	S–C–F	109.5
C–F	1.38158	F–C–F	109.5
S–N	1.77759	C–S–N	115.6
S–O	1.53640	C–S–O	112.6
		N–S–O	106.1
		O–S–O	102.8
		S–N–S	112.5
NEW $[NTf2]^-$			
C–S	1.840	S–C–F	111.8
C–F	1.380	F–C–F	107.1
S–N	1.570	C–S–N	115.6
S–O	1.420	C–S–O	102.6
		N–S–O	113.6
		O–S–O	118.5
		S–N–S	125.6
$[OTf]^-$			
C–S	1.818	F–C–S	111.8
C–F	1.323	F–C–F	107.1
S–O	1.442	O–S–O	115.3
		C–S–O	102.6

EPSR Fits

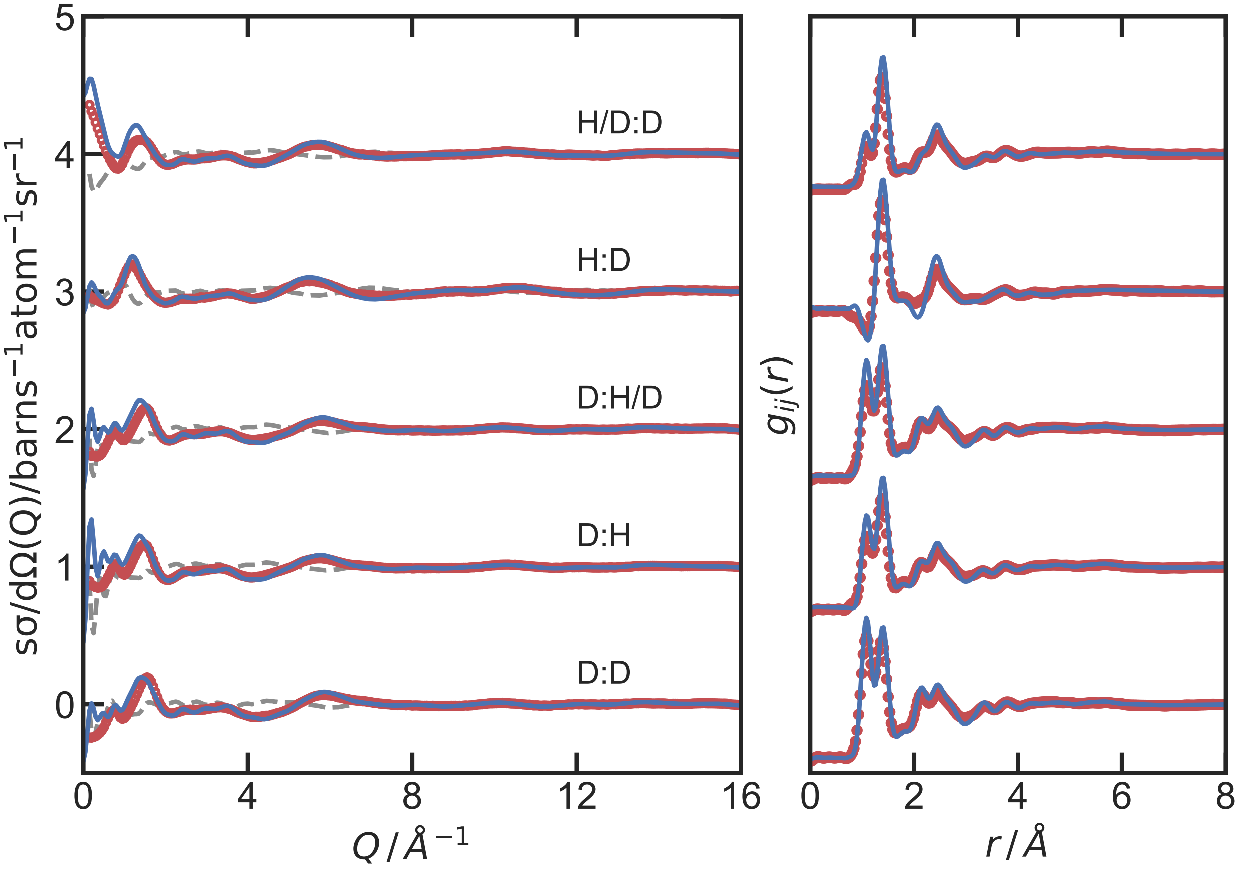

Figure S4: Comparison of the structure factors (left) and transformations to real space (right) for the experimental (symbols) and EPSR modeled (solid) data for the isotopically labelled 2:1 [Me−3-Pic][NTf$_2$]:phenol liquid. Residual differences between the experimental and simulated data are shown by the dashed lines. The curves have been shifted for clarity and are labelled with the isotopic composition of the components.

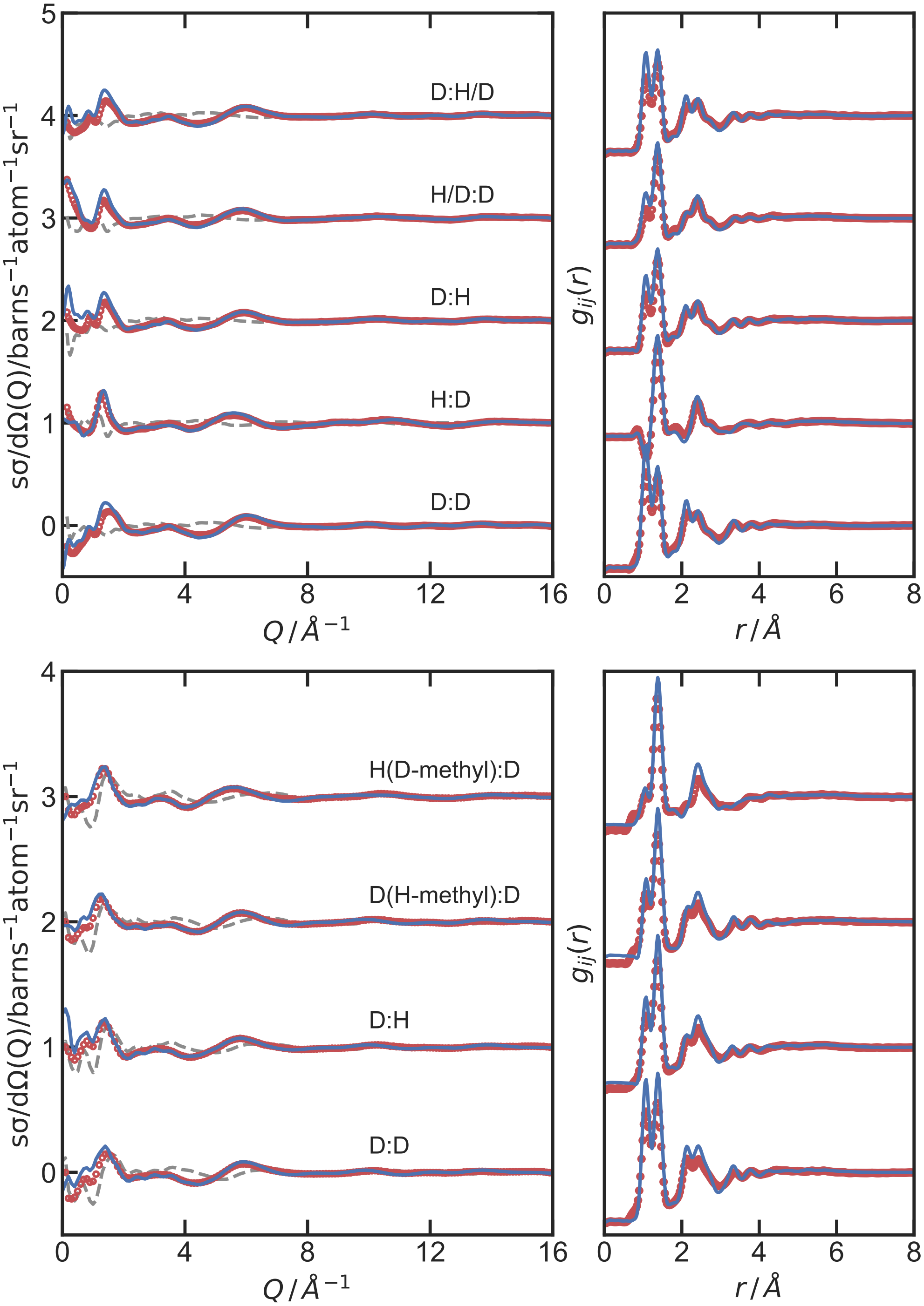

Figure S5: Comparison of the structure factors (left) and transformations to real space (right) for the experimental (symbols) and EPSR modeled (solid) data for the isotopically labelled 2:1 IL:phenol liquids, [Me-Py][OTf] (top) and [Me−Py][NTf$_2$] (bottom). Residual differences between the experimental and simulated data are shown by the dashed lines. The curves have been shifted for clarity and are labelled with the isotopic composition of the components.

Centre of Mass Radial Distribution Functions (COM) RDFs

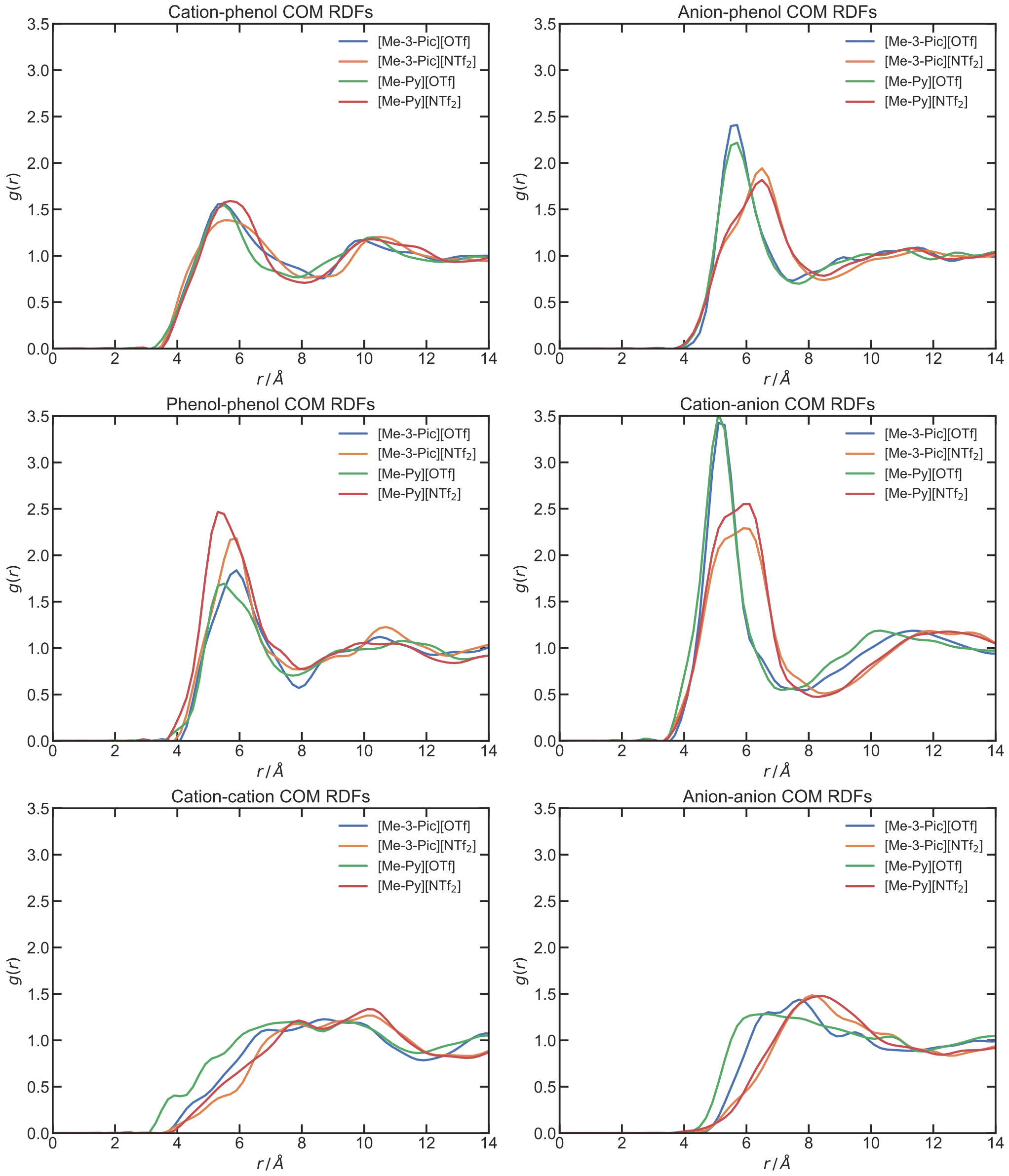

Figure S6: Centre of mass RDFs for each species-species pairs for each system. Centre of mass is defined as the centre of the aromatic ring for cations and phenol molecules, the C–S bond in $[OTf]^-$ and the S–N–S backbone for$[NTf_2]^-$ anions.

Partial Radial Distribution Functions (pRDFs)

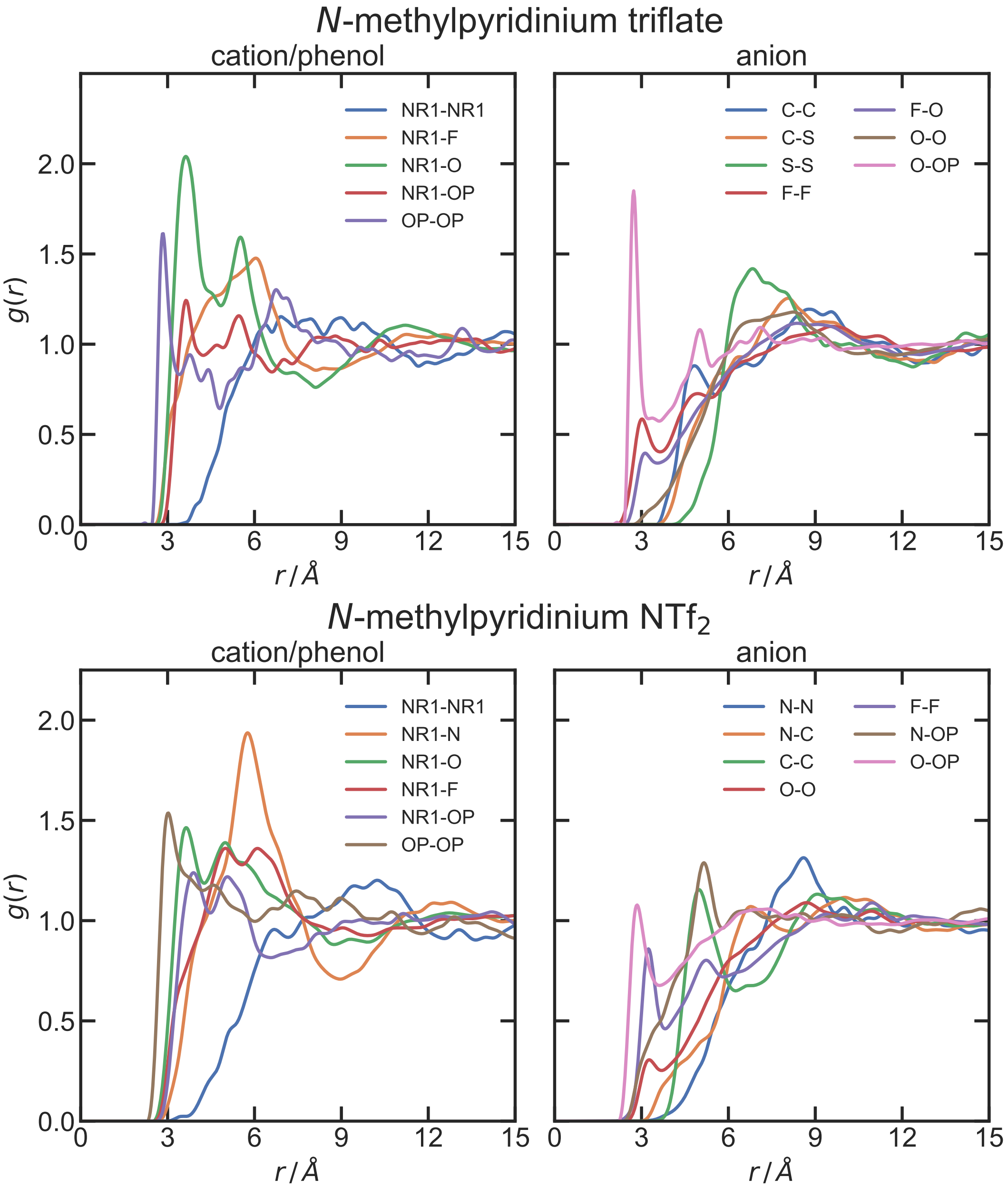

Figure S7: Atom-centred pRDFs for [Me-Py][OTf] & [Me – Py][NTf_2]

Structural and Hydrogen Bonding Analysis

Analysis of hydrogen bonding in the four IL:phenol systems was done using the COORD, TRIANGLES, CHAINS and CLUSTERS subroutines of EPSR25.

Table S8: Hydrogen bonding interactions for OP···X distributions in the IL:phenol mixtures. Coordination numbers within 3.2 Å and the primary correlation peak (r_{max}) in the pRDF of the OP···X interactions across all IL:phenol mixtures. Distances are given in Å

OP···	[Me-3-Pic][OTf]		[Me−3-Pic][NTf$_2$]		[Me-Py][OTf]		[Me−Py][NTf$_2$]	
	r_{max}	N_{coord}	r_{max}	N_{coord}	r_{max}	N_{coord}	r_{max}	N_{coord}
OP	2.73	1.12±0.37	2.75	1.15±0.36	2.81	1.16±0.37	2.94	1.08±0.27
NR1	3.97	0.02±0.15	3.76	0.02±0.15	3.64	0.02±0.13	3.85	0.02±0.14
O	2.73	0.78±0.53	2.77	0.78±0.57	2.71	0.77±0.55	2.75	0.47±0.55
S	3.85	0.00±0.06	3.95	0.00±0.06	3.89	0.00±0.06	4.01	0.00±0.00
F	2.98	0.25±0.50	3.16	0.31±0.57	3.10	0.34±0.61	3.11	0.47±0.79
N	-	-	2.97	0.05±0.22	-	-	5.10	0.03±0.16

Snapshots from the EPSR models for the four IL:phenol mixtures are shown in Figure S8. Qualitatively, phenol–phenol clusters in the snapshots is more prevalent in the [OTf]$^-$ ionic liquids:phenol systems. This observation is corroborated by the cluster analysis which shows that phenol only clusters are more common than composite (cation + phenol) clusters in [OTf]$^-$ ionic liquids:phenol systems. Both [OTf]$^-$ ionic liquids:phenol mixtures show methyl clustering probabilities significantly higher than [NTf$_2$]$^-$ mixtures. Larger phenol–phenol clusters are also more common in [Me−Py]$^+$ which corroborates the longer COM distances for phenol–phenol RDFs in Table 1 (main text).

Cluster analysis of the four IL:phenol mixtures (Fig. S9) which shows that phenol only clusters are more common than composite (cation + phenol) clusters in [OTf]$^-$ ionic liquids:phenol mixtures. Both [OTf]$^-$ ionic liquids:phenol mixtures show methyl clustering probabilities significantly higher than [NTf$_2$]$^-$ mixtures.

Figure S10 shows angle distribution for hydrogen bonds of the type OP-HO···X, where X = OP, O, or F. In line with the shorter r_{max} values presented in Table S8 and the main text, OP-HO···OP/O show more linear and therefore stronger hydrogen bonds.[S9]

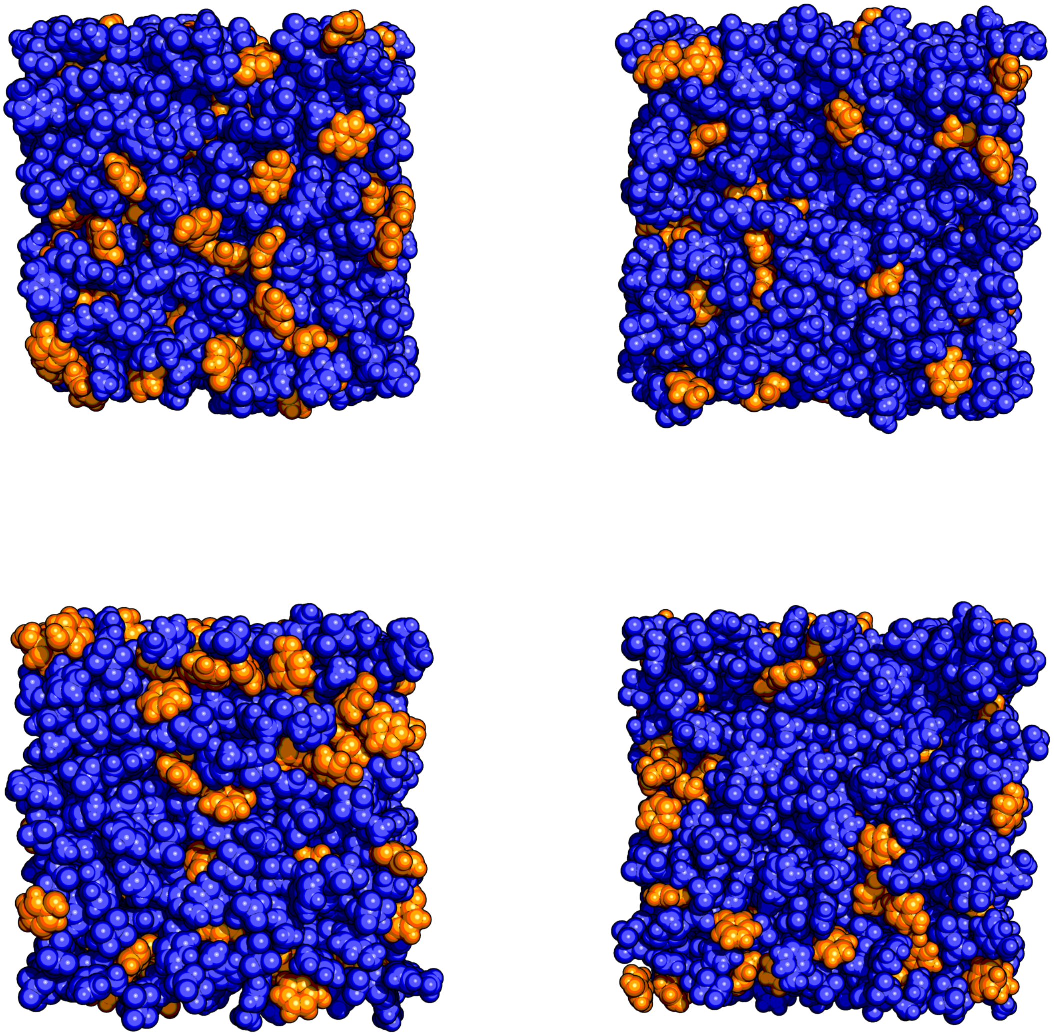

Figure S8: Simulation snapshots of [Me-3-Pic][OTf] (top-left), [Me−3-Pic][NTf$_2$] (top-right), [Me-Py][OTf] (bottom-left), & [Me−Py][NTf$_2$] (bottom-right). The ionic liquid is highlighted in blue and phenol in orange. Corresponding cluster distributions are shown (centre) along with hydrogen bonded chain length distributions (right).

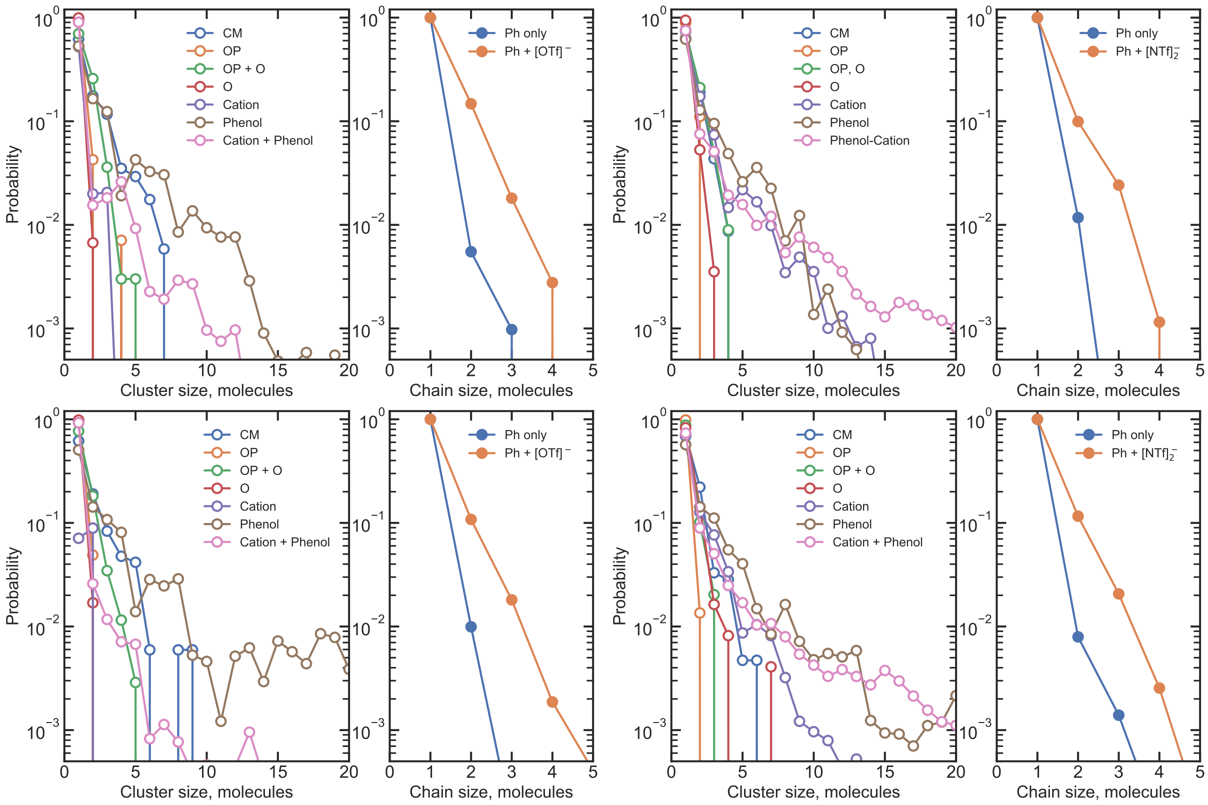

Figure S9: Hydrogen bonding analysis of [Me-3-Pic][OTf] (top-left), [Me−3-Pic][NTf$_2$] (top-right), [Me-Py][OTf] (bottom-left), & [Me−Py][NTf$_2$] (bottom-right). Corresponding cluster distributions are shown (left) along with hydrogen bonded chain length distributions (right).

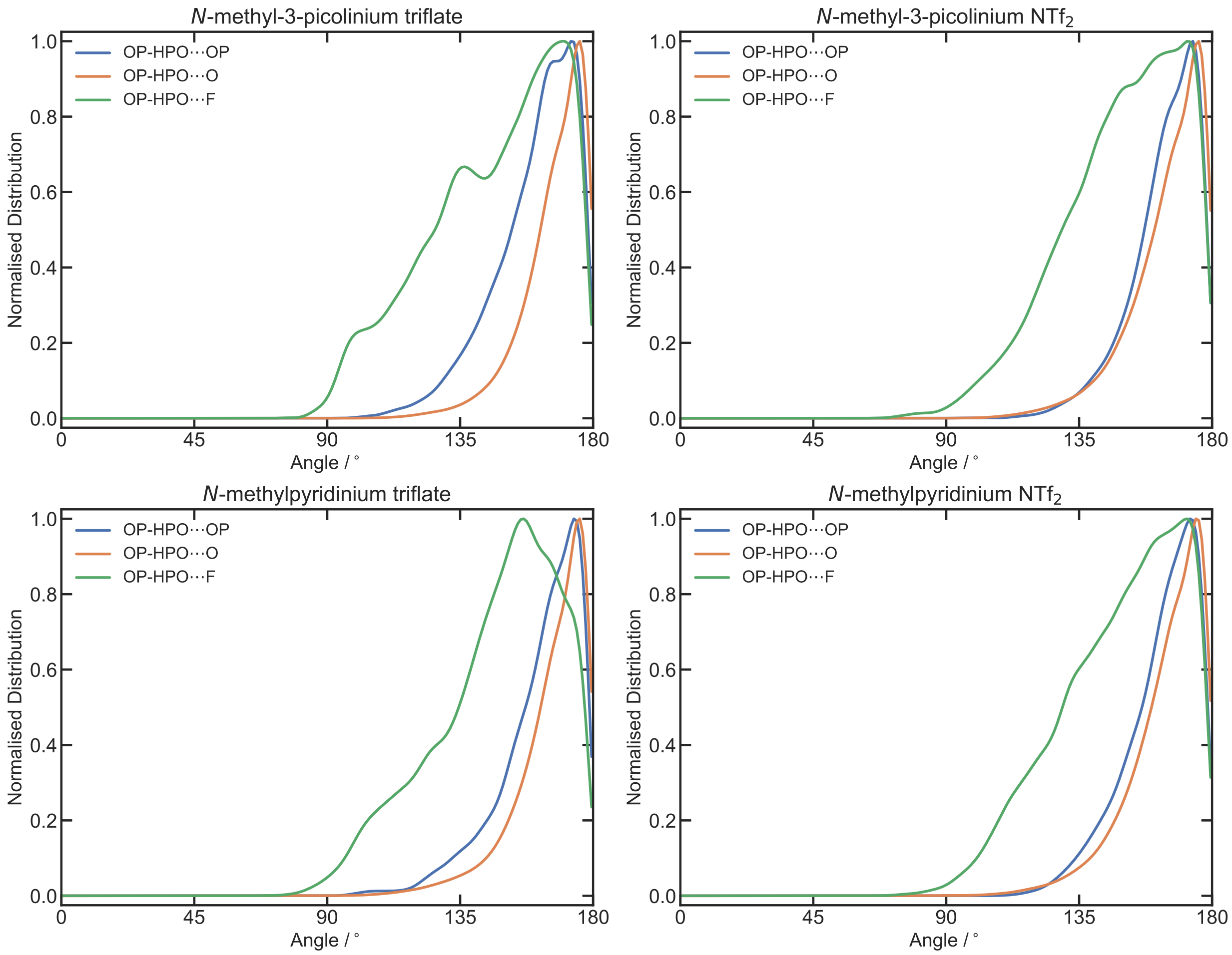

Figure S10: Normalised angle distribution for hydrogen bonds as per Table 3 (main text). Angles are defined between OP-HPO$\cdots$X where X=OP, O, or F atomic triplets.

References

(S1) Turner, A. H.; Holbrey, J. D. *J. Solution Chem.* **2015**, *44*, 621–633.

(S2) Pauling, L. *J. Am. Chem. Soc.* **1932**, *54*, 3570–3582.

(S3) Burley, S. K.; Petsko, G. A. *Science (80-.).* **1985**, *229*, 23–28.

(S4) Hunter, C. A.; Sanders, J. K. M. *J. Am. Chem. Soc.* **1990**, *112*, 5525–5534.

(S5) Hardacre, C.; Holbrey, J. D.; Mullan, C. L.; Nieuwenhuyzen, M.; Youngs, T. G. A.; Bowron, D. T. *J. Phys. Chem. B* **2008**, *112*, 8049–8056.

(S6) Canongia Lopes, J. N.; Padua, A. A. H. *J. Phys. Chem. B* **2004**, *108*, 16893–16898.

(S7) Sambasivarao, S. V.; Acevedo, O. *J. Chem. Theory Comput.* **2009**, *5*, 1038–1050.

(S8) Jorgensen, W. L.; Maxwell, D. S.; Tirado-Rives, J. *J. Am. Chem. Soc.* **1996**, *118*, 11225–11236.

(S9) Bellamy, L. J.; Pace, R. J. *Spectrochim. Acta* **1966**, *22*, 525–533.